Sublethal effects of photoactive engineered nanomaterials on filamentous bacteriophage infection and *E. coli* gene expression in freshwater

Supplementary Information

Shushan Wu [a], Stefanie Huttelmaier [a], Jack Sumner [a], Erica Hartmann [a], Kimberly Gray [a *]

[a] Department of Civil and Environmental Engineering, Northwestern University, 2145 Sheridan Road, Evanston, IL, 60208

* Corresponding author: Kimberly Gray. Email: k-gray@northwestern.edu.

Contents

List of Tables

List of Figures

Table S1. Summary of literature about effects of ENMs on phage structure and phage infection.

ENMs (Type, size, and concentrations)	Experiment setup		Results	Reference
nZVI (3 types: pristine, partially oxidized, and oxidized; <100 nm; 0.01-10 mg/L)	**Phage**	Phages T4, T7, M13, and MS2	Inactivation observed at 0.1 and 1 mg/L doses. M13 appeared to be the most vulnerable to all forms of nZVI, whereas T7 appeared to be almost completely resistant. Pristine, partially oxidized, and completely oxidized inactivated phages via redox reactions involving virion proteins, reactive species generated upon oxidation, and released iron ions, respectively.	Raza et al. [1]
	Bacteria host	*E. coli* BL21 or C3000		
	ENMs exposure media	TM buffer		
nZVI (50 nm; 20-100 mg/L)	**Phage**	Phages MS2 and PhiX174	High concentration of phage MS2 was completely inactivated by 40 mg/L nZVI at pH=7, while complete inactivation of phage PhiX174 could not be achieved. nZVI destroyed surface protein of phage, causing distortion of shape and rupture of capsid. The primary reason for inactivation was the destruction of nucleic acid. Inactivation of RNA viruses (phage MS2) by nZVI was more effective than DNA viruses (phage PhiX174).	Cheng et al. [2]
	Bacteria host	*E. coli* (ATCC 15597 and ATCC 13706)		
	ENMs exposure media	Nutrient broth		
nZVI (50-100 nm; 10-100 mg/L)	**Phage**	Phage f2	nZVI was more efficient in phage f2 inactivation than commercial iron powder. Phage removal rate increased as nZVI dose and rotation rate increased. pH and O_2 are determinants of phage removal rate. The removal efficiency was higher in aerobic conditions. ROS was the primary mechanism for phage inactivation under aerobic conditions. The interaction between phage and nZVI was the main reason in anaerobic conditions.	Cheng et al. [3, 4]
	Bacteria host	*E. coli* 285		
	Cell culture conditions	Nutrient broth		
Bacterial cellulose-supported nZVI (BC-nZVI) (~ 200 nm; 20-60 mg/L nZVI)	**Phage**	Phage MS2	BC-nZVI prepared with low concentration of $FeSO_4$ dispersed nZVI, reduced agglomeration, delayed oxidation, and reduced the influence of pH on phage inactivation. The inactivation process had two phases: the first 5 min of high efficiency inactivation (main factor affecting removal rate was superoxide and Fe[IV]), followed by slow inactivation (mainly affected by ·OH).	Yuan et al. [5]
	Bacteria host	*E. coli* (ATCC 15597)		
	ENMs exposure media	Nutrient broth		
Fe/Ni nanoparticles (~ 93 nm; 20-80 mg/L)	**Phage**	Phage f2	Fe/Ni NPs were more efficient in phage inactivation than nZVI. Optimal efficiency achieved with Fe:Ni=5:1 and pH=6. The removal efficiency was higher in aerobic conditions than anaerobic and was positively related with rotation rate and negatively related with initial concentration of the phage. NPs dose could increase the removal efficiency of phage f2 but decrease the removal efficiency when the dose was too much because of the aggregation of NPs. High temperature improved the reaction rate at the initial stage (first 5 min) but decreased the removal efficiency due to the accelerated corrosion of iron. The mechanism of phage inactivation was mainly by ROS generated from oxidized iron ions and Ni(0) as catalyst.	Cheng et al. [6]
	Bacteria host	*E. coli* 285		
	ENMs exposure media	Nutrient broth		
	Phage	Phage $T4_5$	Decreased phage lytic performance was observed with SiO_2 (ζ ~ -51 mV) and Fe_3O_4-SiO_2 (ζ ~ -37.6 mV) NPs and increased phage lytic performance was observed with	Stachurska et al. [7]

n-SiO_2, n-TiO_2, n-Fe_3O_4, and TiO_2-SiO_2, Fe_3O_4-SiO_2, SiO_2-Fe_3O_4-TiO_2 NPs (20-120 nm; 0.5-0.05 mg/mL)	**Bacteria host**	*E. coli* K12 C600	other NPs (ζ -25 mV to 36 mV). It can be hypothesized that the nanoparticle charge, negative or positive, is not enough for the phage to attach specifically to the particle. Zeta potential of NPs is of great influence. NPs with ζ < -35 mV bind with tail fibers of phage, decreasing phage infection. NPs with ζ > 35 mV bind with phage head and NPs with ζ in between have nonspecific binding with phage. In both cases, phage lytic performance increased.	
	ENMs exposure media	TM buffer and LB broth		
n-TiO_2 (5-100 nm; 0.05-50 mM)	**Phage**	Engineered phage M13	n-TiO_2 improved adsorption of phage to cell and impaired cell membrane stability, promoting the entry of phage to cell. n-TiO_2 induced intracellular ROS generation which enhanced the expression of pilus-related genes, contributing to phage transduction. 0.5 mM and 20-50 nm n-TiO_2 had greatest effects on transductant formation.	Han et al. [8]
	Bacteria host	*E. coli* TG1		
	ENMs exposure media	PBS buffer		
n-Ag (Uncoated and PVP-coated; 10 nm; 0.025, 0.25, and 1.25 mg/L to bacteria; 10 mg/L to phage)	**Phage**	Phages KL and RG2014	Incubated with uncoated n-Ag reduced 96% phage plaque yield, while PVP-coated n-Ag increased phage infection up to 250%. The inhibitory effect of n-Ag on phage infection was dependent on the binding of metal nanoparticles to exposed positively charged C-terminal amino acid residues on the phage capsid surface.	Gilcrease et al. [9]
	Bacteria host	*K. pneumoniae* and *D. tsuruhatensis*		
	ENMs exposure media	LB broth for bacteria, SMG/TM buffer for phage		
n-Ag (Uncoated, 6-10 nm; 0.01-10 mg/L)	**Phage**	Engineered phage M13	n-Ag improved the transduction efficiency of planktonic bacteria by increasing membrane permeability induced by intracellular oxidative stress. Phage-specific recognition and biological binding facilitated the bacterial adhesion of n-Ag. 0.1 mg/L n-Ag had the largest effect of increasing transductants to 4-fold. Moreover, n-Ag exposure led to the formation of thinner biofilms, which further increased phage-mediated the ARGs dissemination in microplastic-attached biofilms.	Zhang et al. [10]
	Bacteria host	*E. coli* XL1-blue		
	ENMs exposure media	2x yeast extract tryptone medium		
n-CuO (<50 nm; 1, 10, 50 mg/L)	**Phage**	-	n-CuO induced lysogenic bacteriophage infection in the bacteria. n-CuO also decreased denitrification gene expression and up-regulated gene expression for copper resistance, resistance-nodulation-division, P-type ATPase efflux, and cation diffusion facilitator transporters.	Guo et al. [11]
	Bacteria host	*P. aeruginosa* PAO1		
	ENMs exposure media	Glycerol modified M9 medium		
Cu and Ag loaded TiO_2 nanowire membrane (using n-TiO_2 P25)	**Phage**	Phage MS2	Enhanced photo-activated bactericidal and virucidal activities were obtained by nanowire membranes with effects: Cu-Ag-TiO_2> Ag-TiO_2>TiO_2>Cu-TiO_2. Cu-Ag-TiO_2 membrane achieved an E. coli removal of 7.68 log and bacteriophage MS2 removal of 4.02 log under 254 nm UV irradiation after 30 minutes.	Rao et al. [12]
	Bacteria host	*E. coli* (ATCC 15597)		
	ENMs exposure media	PBS buffer; UV irradiation		
n-Ag (PVA-capped, ~ 21 nm; 1-5 mg/L); n-ZnO (~ 39 nm; 5-20 mg/L)	**Phage**	Phage MS2	Prior exposure to n-Ag or Ag^+ ions did not inactivate the bacteriophage. When bacteria were exposed to MS2 and NPs simultaneously, both n-Ag (5 mg/L) and n-ZuO (20 mg/L) increased phage infection by 2–6 orders of magnitude via plaque count.	You et al. [13]
	Bacteria host	*E. coli* (ATCC 15597)		
	ENMs exposure media	PBS buffer		
Iron-doped apatite nanoparticle (FeNP) (100 nm; 7.5 and 12.5 mM)	**Phage**	Phages Bxz1 and P2	Exposure to NPs of bacteria and bacteria/phage increased phage infection 11%-24% via plaque count. NPs' accumulation towards poles of cells possibly made receptor	Nickel et al. [14]
	Bacteria host	*M. smegmatis* and *E. coli* A λ and B		

	ENMs exposure media	7H9 mixture and LB broth	sites more available for phage absorption and infection. NPs affected cell outer layer, making cells less resistant to phage infection.	
Effects of photoactive ENMs under light on phage				
n-TiO_2 (20 nm; 0.5 mM) **Light source:** UV irradiation (365 nm; 150 μW/cm^2)	**Phage**	Engineered phage M13	n-TiO_2 photoexcitation promoted phage transduction efficiency and transductant formation greatly. Extracellular ROS damaged cell membrane and intracellular ROS induced pilus synthesis, contributing to phage invasion. Excessive UV irradiation led to cell death and phage inactivation and consequently, reduced phage transduction efficiency.	Xiao et al. [15]
	Bacteria host	*E. coli* TG1		
	ENMs exposure media	PBS buffer		
n-TiO_2 (20-40 nm anatase; 0-80 mg/L) **Light source:** UVA light (120 μW/cm^2, 1 hr)	**Phage**	Engineered phage M13	In the dark, n-TiO_2 exhibited an antagonistic effect on phage transduction promoted by HA due to its adsorption on HA. Under illumination, the combination of n-TiO_2 and HA synergistically facilitates phage transduction due to increased ROS generation ($O_2^{\bullet-}$) that promoted the membrane permeability and intensified intracellular oxidative stress.	Zhang et al. [16]
	Bacteria host	*E. coli* XL1-blue		
	ENMs exposure media	2x yeast extract tryptone medium		
n-TiO_2 (25 nm anatase; 10 mg/L) **Light source:** ambient light	**Phage**	Phage MS2	Low concentration of n-TiO_2 inactivated phage MS2 slightly with or without ambient light at room temperature. The presence of quartz sand hindered the inactivation, probably by blocking the migration of electrons to TiO_2 NPs and hence reducing possible ROS production, which in turn decreased MS2 inactivation. PBS hindered phage inactivation by n-TiO_2 because of possible increased MS2 aggregation in PBS solution due to binding of phosphate to positively charged lysine, a hydrophilic amino acid residue found at MS2 proteins.	Syngouna et al. [17]
	Bacteria host	*E. coli* (ATCC 15597)		
	ENMs exposure media	Distilled deionized water and PBS buffer		
n-TiO_2 (25 nm P25; 1 g/L) **Light source:** UV-A, 10W and UV-B, 8W; 0.14 mW/cm^2	**Phage**	Phage MS2	n-TiO_2 enhanced the inactivation of phage MS2 and murine norovirus (MNV) by UV-A. The addition of TiO_2 increased the efficacy of UV-B disinfection for inactivating MS2, but did not significantly increase the inactivation of MNV, possibly due to the difference in genome size.	Lee et al. [18]
	Bacteria host	*E. coli* (ATCC 15597)		
	ENMs exposure media	Groundwater and PBS buffer		
n-TiO_2 (~20 nm P25; 0.01-0.2 kg/m^3) **Light source:**20W black light lamp, 8-23 W/m^2	**Phage**	Phage MS2	Significant inactivation of phage MS2 took place only in combination with TiO_2 and light irradiation. The effect exhibited linear decrease with the passage of irradiation time. The apparent rate constant for inactivation was approximately proportional to average light intensity and increased with an increase in TiO_2 concentration. pH dependency of the inactivation rates was associated with the electrostatic properties of TiO_2 and MS2 surfaces.	Koizumi et al. [19]
	Bacteria host	*E. coli* (ATCC 15597)		
	ENMs exposure media	Distilled water		
Cu-TiO_2 nanofibers (100-200 nm diameter; 25-150 mg/L) **Light source:** Xenon lamp >400 nm	**Phage**	Phage f2	The nanofiber showed great inactivation abilities to *E. coli* and phage f2 under visible light. In the test range, initial pH did not affect the final inactivation efficiency. The removal efficiency of bacteriophage f2 increased with the increase of nanofiber concentration, light intensity and temperature, but decreased with the increase of initial virus concentration. Free ROS in the bulk phase played a crucial role in phage f2 inactivation, while competitive adsorption in the mixed system played a certain role in *E. coli* inactivation.	Zheng et al. [20]
	Bacteria host	*E. coli* 285		
	ENMs exposure media	Sterilized water with HCl and NaOH		

Table S2. Characterization of n-TiO_2 P25 and n-Ag [21].

ENMs Type and name	Purity [a]	Primary particle size (nm) [b]	In MOPS		In LMW		Crystallinity [e]
			Aggregate size (nm) [c]	Mean zeta potential (mV) [d]	Aggregation size (nm) [c]	Mean zeta potential (mV) [d]	
n-TiO_2 P25	≥ 99.5%	22.4	1057 ± 73	- 22.6	894 ± 92	-14.4 [22]	84% Anatase, 16% Rutile
n-Ag (Citrate stabilized)	99.99%	10.8 [c]	37 ± 7	-64.0	28 ± 5	-59.8	Crystalline

[a] From manufacturers' websites. [b] From XRD based on Scherrer equation. [c] Measured by dynamic light scattering (DLS) by Zetasizer, presented as average ± standard deviation (n=3). The aggregate size of n-TiO_2 was measured with the concentration of 20 mg/L. The aggregate size of n-Ag was measured with the concentration of 1 mg/L. [d] Measured by Zetasizer. [e] From XRD.

Table S3. Targeted F-pili and membrane protein genes and primers.

Name	Primer sequences (5'-3')		Melt temperature	Function
traA [a]	**Forward**	AGT GTT CAG GGT GCT TCT	88.5 °C	Encoding F pilin
	Reverse	GCC TTA ACC GTG GTG TT		
traX [a]	**Forward**	GCG GAA GAC AGA ATG GAA C	88.5 °C	Affecting F pilin acetylation
	Reverse	CAG CAC CGT CAT CAC AAG G		
traV [a]	**Forward**	AGT GTT CAG GGT GCT TCT	89.5 °C	Affecting F pilin assembly
	Reverse	GCC TTA ACC GTG GTG TT		
ompF [b]	**Forward**	GAA CTT CGC TGT TCA GTA CC	85.5 °C	Receptor for phage f1
	Reverse	CGT ACT TCA GAC CAG TAG CC		
tolAIII [c]	**Forward**	GCT ATC GAA AGT AAG TTC TAT GAC G	83.5 °C	Receptor for phage f1
	Reverse	CAA CGC AGCC TGA CAA AG		
rpoA [a]	**Forward**	GGA AAC CAA CGG CAC AAT C	85 °C	Housekeeping gene (internal control)
	Reverse	GCA GTT AGC AGA GCG GAC AG		

Notes: [a] Primers adopted from Han et al. [8].
[b] Primer adopted from Viveiros et al. [23].
[c] Primer designed using the IDT PrimerQuest Tool.

Table S4. Pearson's correlation coefficient (r) between phage infection and outer membrane permeability [21] under different ENM treatments.

ENMs	r	Interpretation
n-TiO_2 P25	0.203	Weakly, positively related
n-Ag	0.34	Moderately, positively related
ENM mixtures	-0.242	Weakly, negatively related

Table S5. A qualitative summary of ENMs effects on cell surface structures, gene expression, and phage infection.

Phenomena		Under simulated sunlight irradiation				Under dark			
		n-TiO_2	n-Ag	ENM mixtures		n-TiO_2	n-Ag	ENM mixtures	
				Compared to n-Ag	Compared to no-ENMs			Compared to n-Ag	Compared to no-ENMs
Outer membrane permeability		+	+	++	+++	0	0	0	0
Phage infection		+	+	-	0	0	+	-	0
F-pili related genes	*traA*	0	+	0	+	0/-	0/+	0	+
	traX	+	+	++	+++	0/-	0/-	0	0
	traV	+	+	++	+++	0/-	0/-	0	0
Membrane protein genes	*ompF*	+	++	0	+++	0/+	+	0	+
	tolAIII	0	0	++	+++	0	0/-	0	0
Pili/F-pili density		+	+	+		0	0	0	
Zeta potential		Less negative	Less negative	More negative	Less negative	Less negative	Less negative	More negative	Less negative

Note: "+" represents a promoting effect, "0" represents negligible or no significant effect, and "-" represents a suppressing/inhibiting effect.

(a)

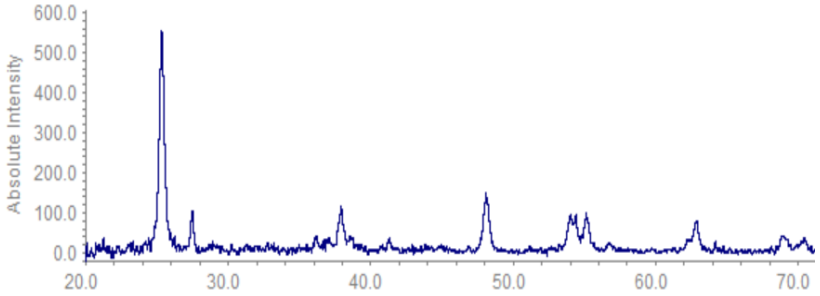

(b)

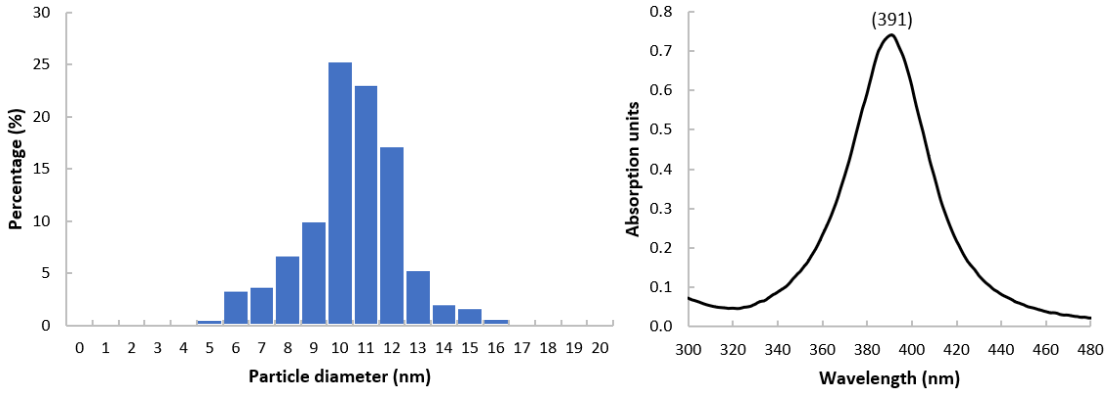

(c)

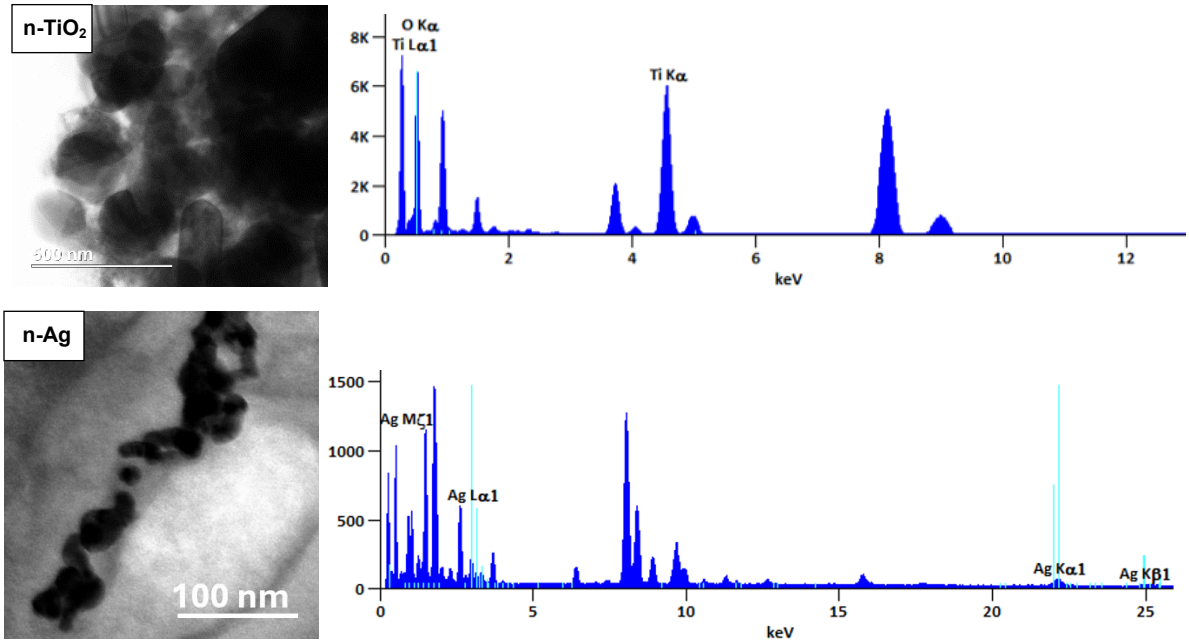

Figure S1. Characterization of n-TiO_2 P25 and n-Ag: (a) X-ray diffractogram (XRD) of n-TiO_2 [21], (b) size distribution and UV−vis spectra of n-Ag [21], and (c) TEM and EDS graphs of n-TiO_2 and n-Ag.

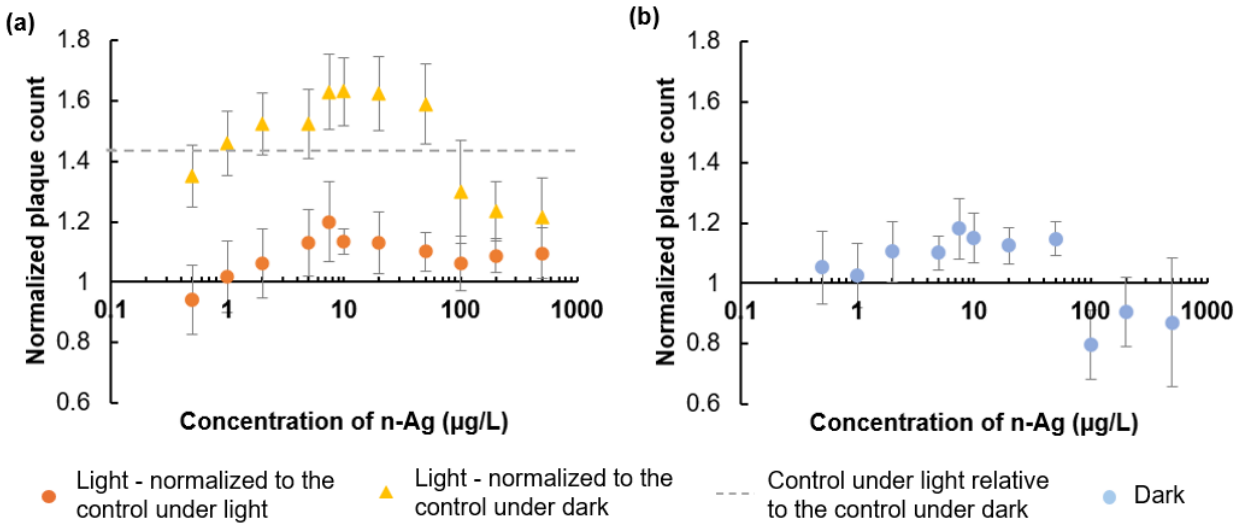

Figure S2. Effects of low concentrations (0-500 μg/L) of n-Ag on phage f1 infection under (a) light and (b) dark. The plaque counts of ENMs-free samples (control) under light or dark were set to 1 and the other results were normalized to the control as described in the legend.

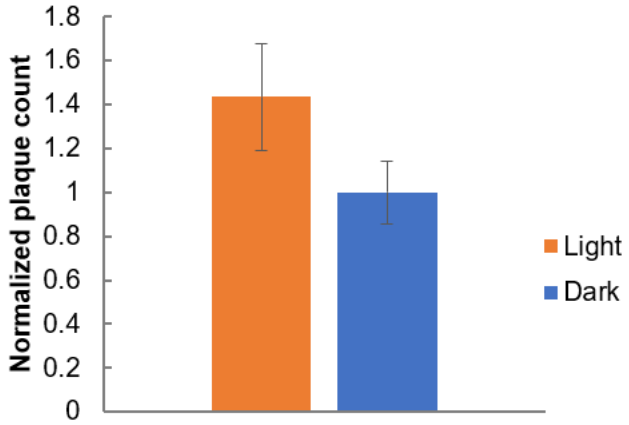

Figure S3. Effect of light on phage f1 infection. The plaque counts of samples under dark were set to 1 and the plaque counts under light were normalized accordingly.

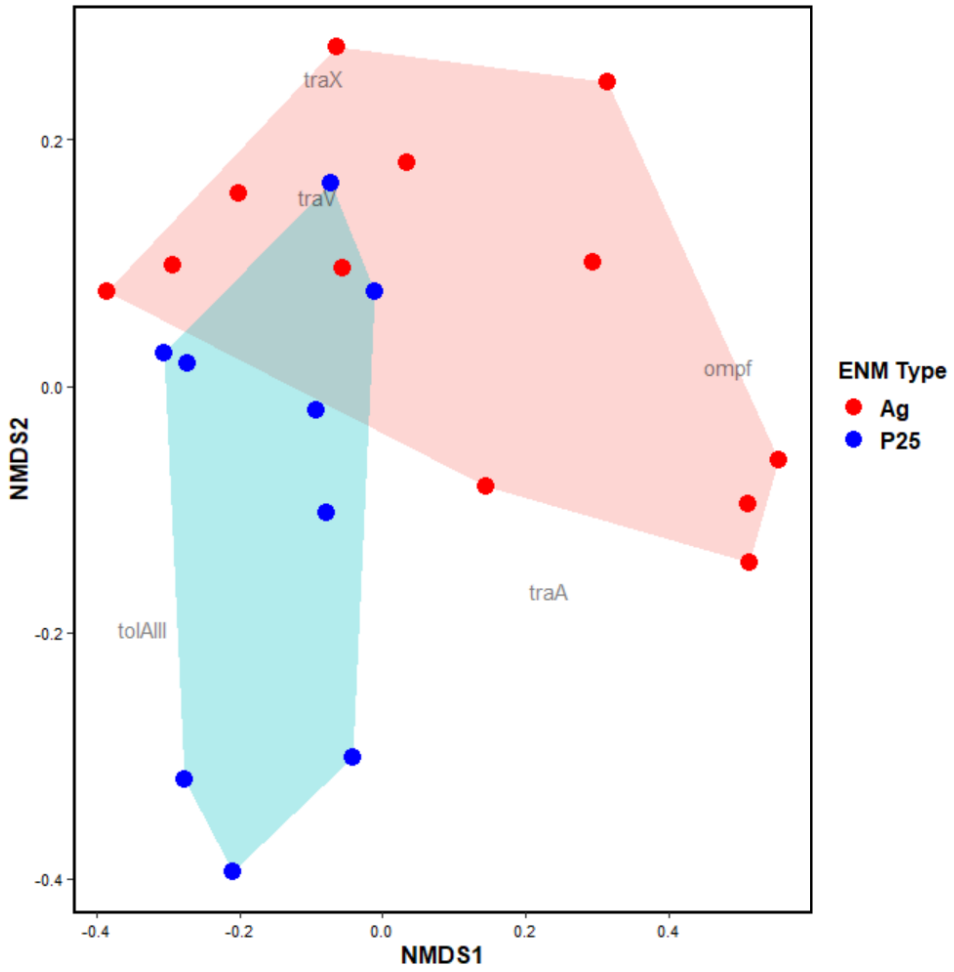

Figure S4. NMDS plot of gene expression data of samples treated with individual ENM (n-Ag or n-TiO_2 P25), stress value = 0.089. The label (*traA*, *traV*, *traX*, *ompF*, and *tolAIII*) is positioned at the centroid of the data for each gene. P25 = n-TiO_2 P25.

Interpretation: The centroids of *traX* and *traV* are closer, indicating high similarity between *traX* and *traV* gene expression data and strong association between the two genes. The centroids of *tolAIII*, *traA*, and *ompF* are far apart, indicating dissimilarity and weak association among those data.

Considering the position of the two clusters formed by different ENM treatment, samples exposed to n-Ag form a cluster (in light red) that covers *traX*, *traV*, and *ompF* centroids and is close to the *traA* centroid but is far from the *tolAIII* centroid; samples exposed to n-TiO_2 P25 form a cluster (in light blue) that covers the *traV* centroid and is close to *traX*, *tolAIII*, and *traA* centroids but is far from the *ompF* centroid. The relative position between clusters and centroids shows that *tolAIII* and *ompF* gene expression data are less similar to the F-pili gene expression data, indicating weak association between *tolAIII* and *ompF* genes and F-pili-related genes. The observations correspond to the results in Section 3.2.1 and the qualitative summary in Table 3.

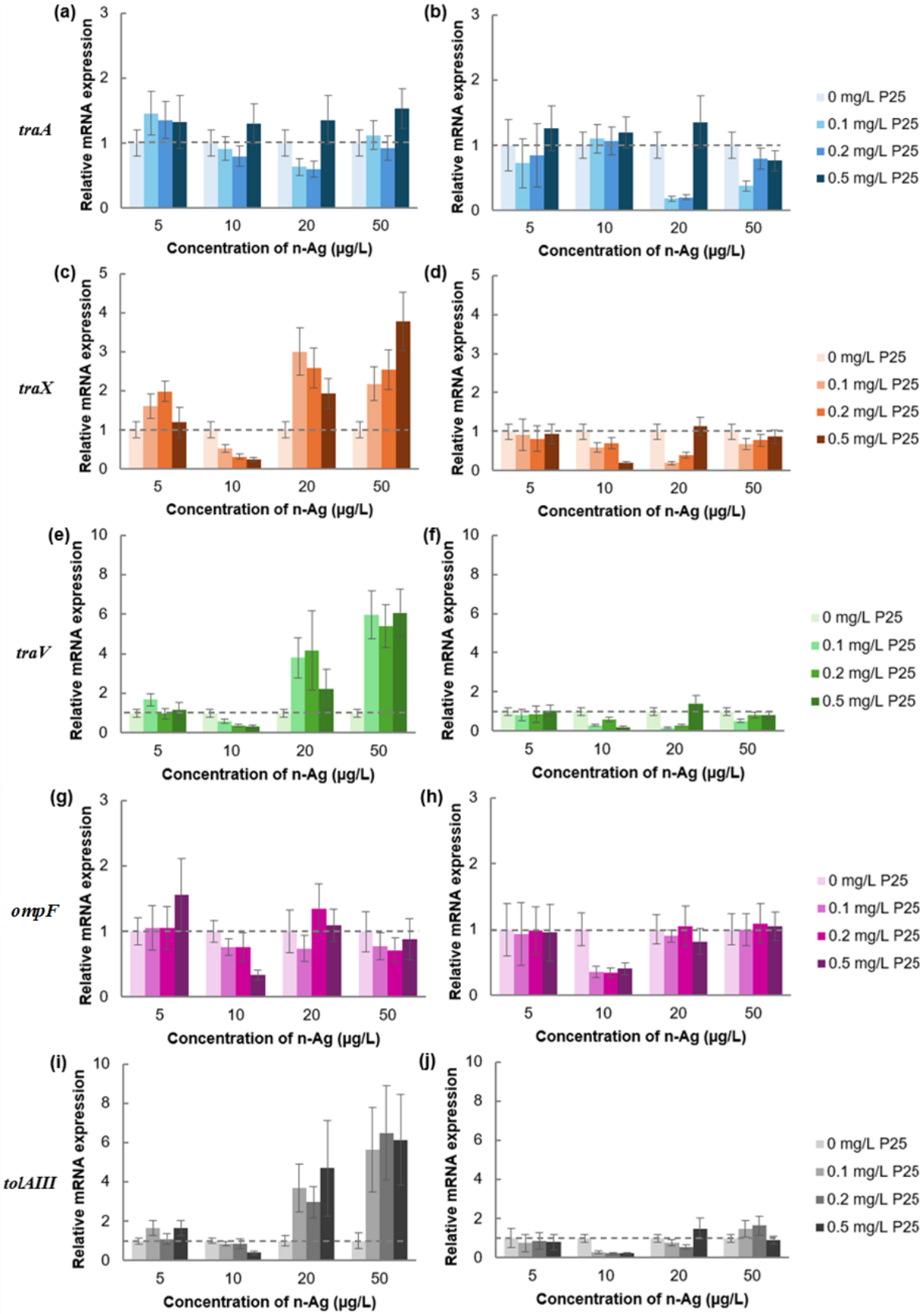

Figure S5. Effects of low concentrations of n-TiO_2 + n-Ag mixtures on *E. coli* genes expression under light (a, c, e, g, and i) and dark (b, d, f, h, and j) relative to n-Ag-only control. The dash lines mark the reading of 1, which is the relative mRNA expression of n-Ag-only control at each n-Ag concentration (the lightest color bars). A value of 0.5-1 indicates no significant change compared to the control. P25 = n-TiO_2 P25.

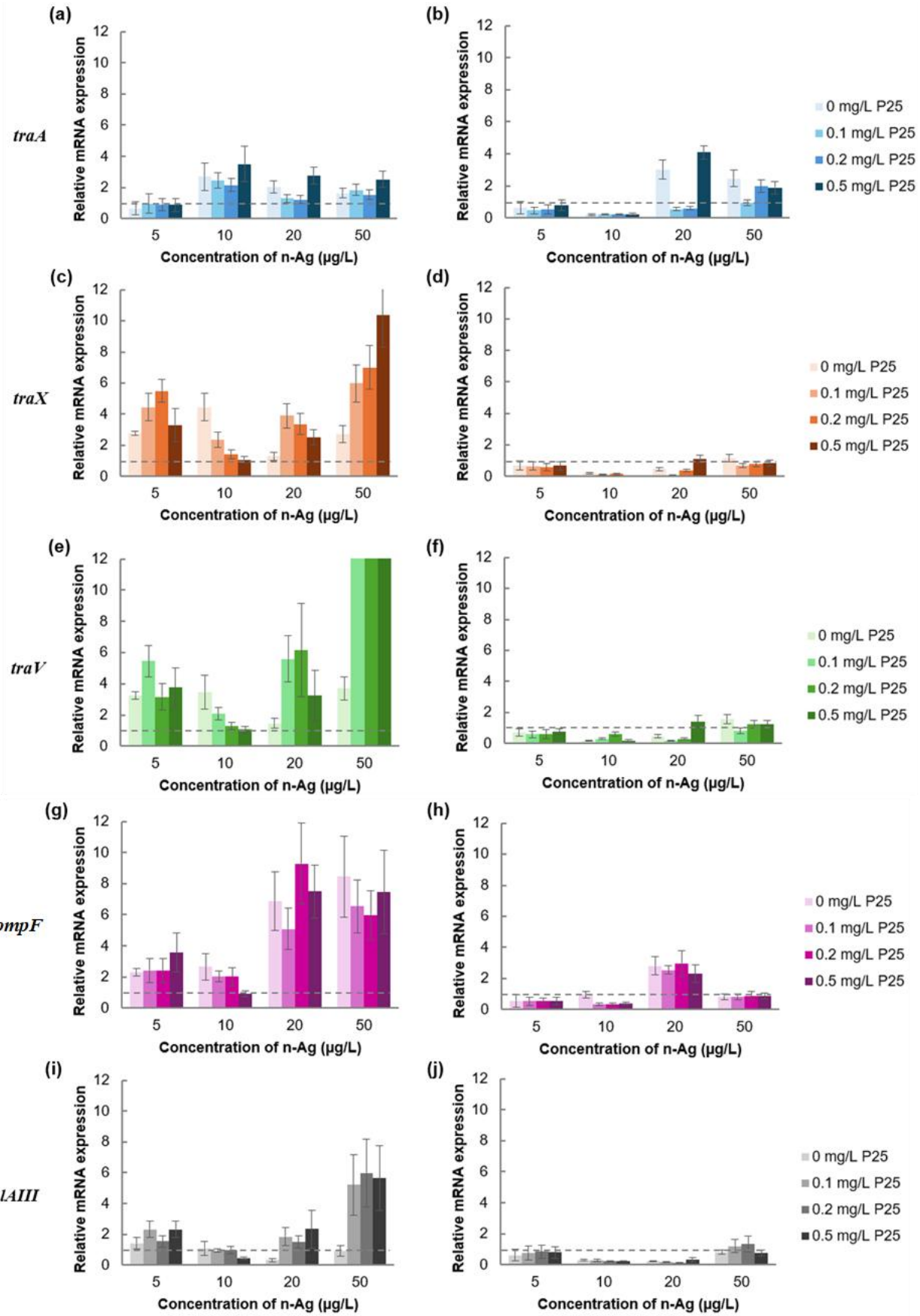
(a)
(b)
(c)
(d)
(e)
(f)
(g)
(h)
(i)
(j)
traA
traX
traV
ompF
tolAIII
Relative mRNA expression
Concentration of n-Ag (μg/L)
0 mg/L P25
0.1 mg/L P25
0.2 mg/L P25
0.5 mg/L P25

(m) Under light

n-Ag (µg/L)	n-TiO_2 P25 (mg/L)	*traA*	*traX*	*traV*	*ompF*	*tolAIII*
0	0	1	1	1	1	1
	0.1	1.2	1.6	1.6	1.7	0.8
	0.2	0.8	2.2	2.1	1.7	1.1
	0.5	0.9	0.5	1.0	1.3	1.0
5	0	0.7	2.8	3.3	2.3	1.4
	0.1	1.0	4.5	5.5	2.4	2.3
	0.2	0.9	5.5	3.2	2.4	1.5
	0.5	0.9	3.3	3.8	3.6	2.3
10	0	2.7	4.5	3.5	2.7	1.1
	0.1	2.5	2.4	2.1	2.0	0.9
	0.2	2.2	1.4	1.3	2.0	1.0
	0.5	3.5	1.1	1.1	0.9	0.4
20	0	2.0	1.3	1.5	6.9	0.3
	0.1	1.3	3.9	5.6	5.1	1.9
	0.2	1.2	3.4	6.1	9.3	1.5
	0.5	2.8	2.5	3.2	7.5	2.3
50	0	1.6	2.7	3.7	8.4	0.9
	0.1	1.9	6.0	22.2	6.5	5.2
	0.2	1.5	7.0	20.1	6.0	6.0
	0.5	2.5	10.4	22.5	7.4	5.6

(n) Under dark

n-Ag (µg/L)	n-TiO_2 P25 (mg/L)	*traA*	*traX*	*traV*	*ompF*	*tolAIII*
0	0	1	1	1	1	1
	0.1	0.4	0.2	0.4	1.6	0.4
	0.2	0.6	0.6	0.9	1.3	0.9
	0.5	0.8	0.9	0.7	1.4	0.8
5	0	0.6	0.7	0.7	0.6	0.6
	0.1	0.5	0.7	0.6	0.5	0.8
	0.2	0.5	0.6	0.6	0.6	0.8
	0.5	0.8	0.7	0.8	0.5	0.8
10	0	0.2	0.2	0.2	1.0	0.3
	0.1	0.2	0.1	0.3	0.4	0.3
	0.2	0.2	0.2	0.6	0.3	0.2
	0.5	0.2	0.0	0.2	0.4	0.2
20	0	3.0	0.5	0.5	2.8	0.2
	0.1	0.5	0.1	0.2	2.5	0.2
	0.2	0.6	0.4	0.3	3.0	0.1
	0.5	4.1	1.1	1.4	2.3	0.3
50	0	2.5	1.2	1.6	0.8	0.8
	0.1	0.9	0.7	0.8	0.8	1.2
	0.2	2.0	0.8	1.3	0.9	1.3
	0.5	1.9	0.9	1.2	0.9	0.7

<0.5	0.5-1.0	1.0-2.0	2.0-4.0	>4.0
Down-regulation	No effect	Up-regulation		

Figure S6. Relative *E. coli* gene expression exposed to the ENM mixtures under light (a, c, e, g, and i) and dark (b, f, h, and j) compared to no-ENMs control. P25 = n-TiO_2 P25. The dash lines mark the reading of 1, which is the relative mRNA expression of bacteria without ENMs under light or dark. The values of *traV* gene expression containing 50 µg/L n-Ag are all above 15 (the last set of bars in Figure S6-e). A value of 0.5-1 indicates no significant change compared to the control. (m) and (n) are heatmaps.

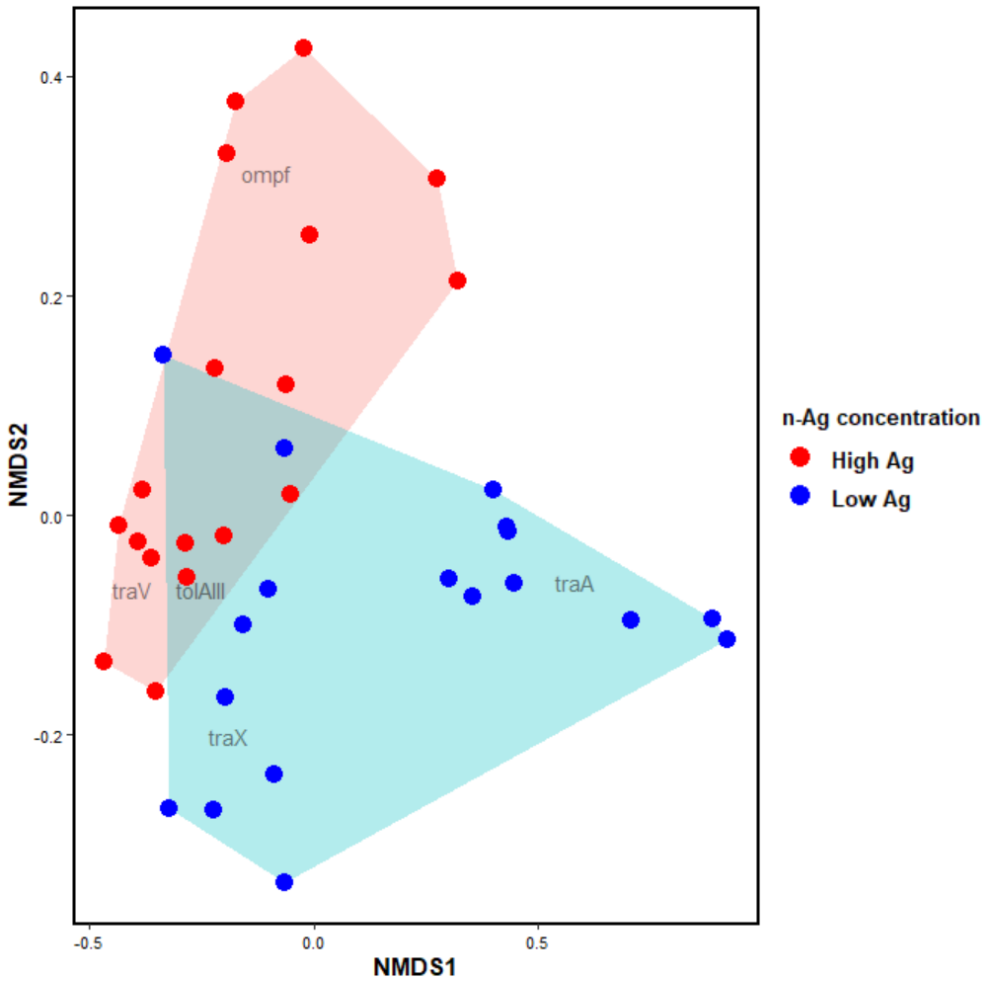

Figure S7. NMDS plots of gene expression data of samples treated with the ENM mixtures, stress value = 0.086. The label (*traA*, *traV*, *traX*, *ompF*, and *tolAIII*) is positioned at the centroid of the data for each gene. "High Ag" represents n-Ag concentrations of 20-50 µg/L, and "Low Ag" represents n-Ag concentrations of 5-10 µg/L.

Interpretation: Clusters are formed mainly with respect to n-Ag concentration range in the binary ENM mixtures. Data in the "High Ag" cluster (in red, samples exposed to the binary ENM mixtures with high n-Ag concentrations) are more concentrated and closer to each other, while data in the "Low Ag" cluster (in blue, samples exposed to the binary ENM mixtures with high n-Ag concentrations) are further apart from each other, indicating stronger similarity and association between data in the "High Ag" cluster and relative weaker association between data in the "Low Ag" cluster.

Considering the position of centroids, the *traX*, *traV*, and *tolAIII* centroids are closer to each other, compared to the other two centroids, indicating high similarity between *traX*, *traV*, and *tolAIII* gene expression data. The observations correspond to the results in Section 3.2.2 and the qualitative summary in Table 4.

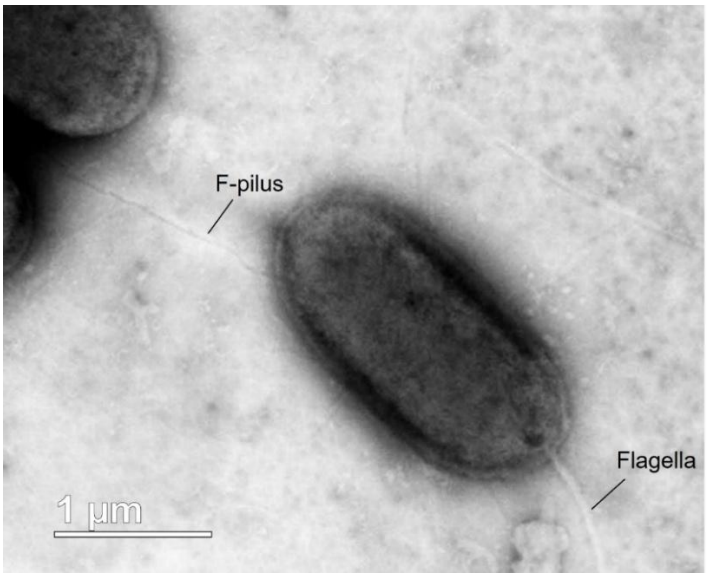

Figure S8. S/TEM image of F-pilus connecting two *E. coli* cells, possibly in conjugation.

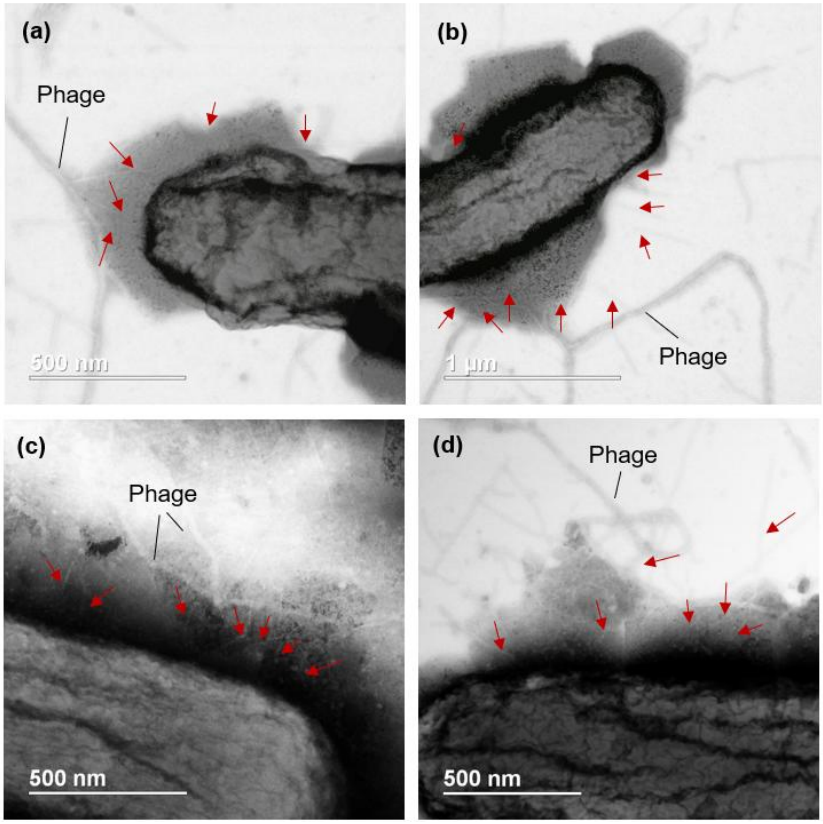

Figure S9. S/TEM images of *E. coli* pre-treated with ENMs in dark and infected with phage f1: (a) control without any ENMs, (b) exposed to 0.2 mg/L n-TiO_2, (c) exposed to 50 µg/L n-Ag, and (d) exposed to 0.2 mg/L n-TiO_2 and 50 µg/L n-Ag mixture. The red arrows point to the pili/F-pili that are relatively difficult to observe on the bacteria.

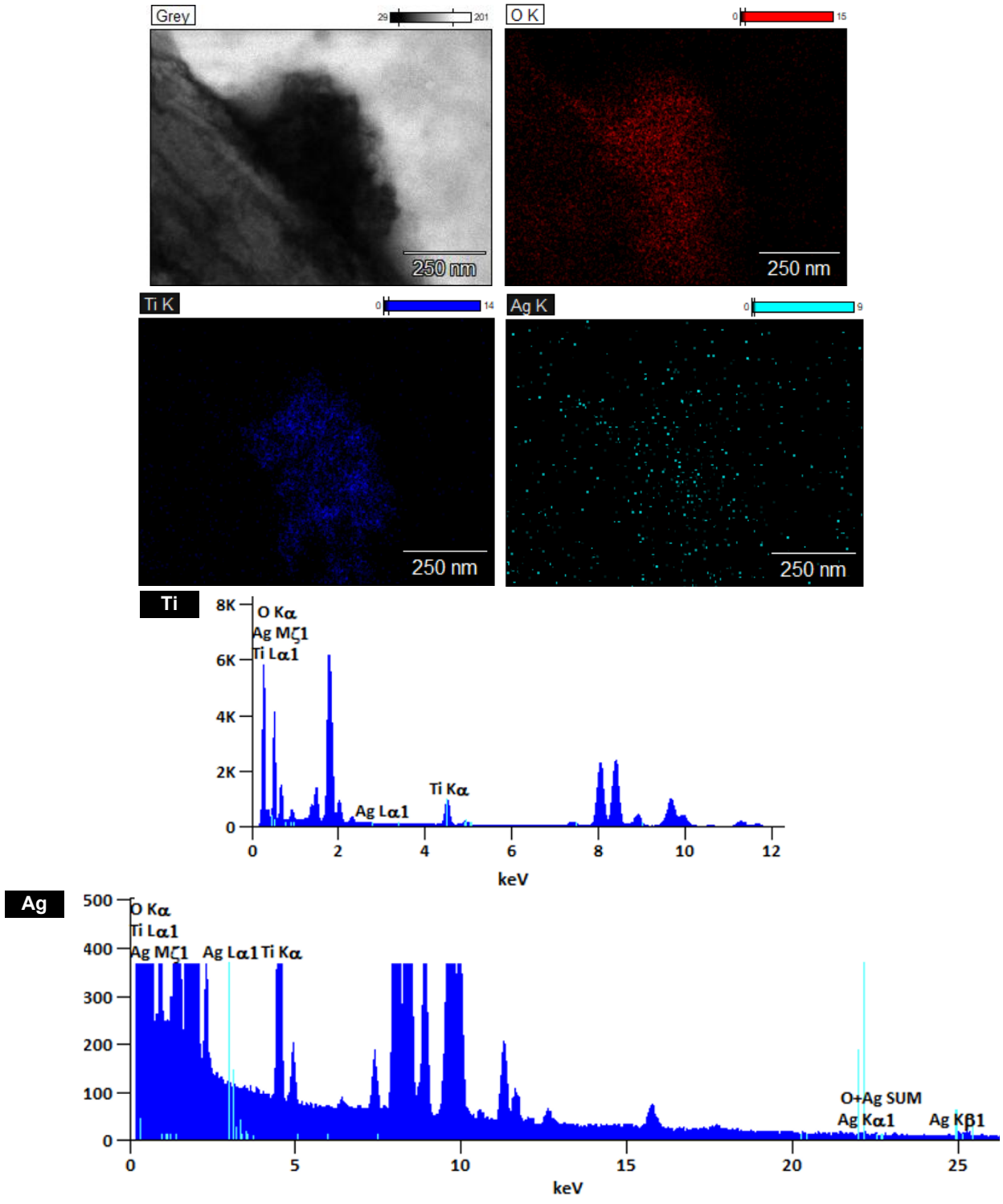

Figure S10. EDS analysis of the n-TiO_2 (0.2 mg/L) and n-Ag (50 µg/L) mixture attached to the *E. coli* cell.

(a)

P25 (mg/L)	0.1	0.2	0.5	1	10
Aggregate size (nm)	466±34	503±3	546±28	791±2	1423±39

(b)

ENMs Concentration		n-Ag (µg/L)				
		50	20	10	5	0
P25 (mg/L)	0.5	382 (±15)	423 (±10)	227 (±1)	370 (±0)	523 (±20)
	0.2	431 (±14)	357 (±3)	317 (±5)	522 (±12)	446 (±22)
	0.1	299 (±15)	444 (±27)	492 (±10)	394 (±49)	402 (±13)

	<400
	400-500
	>500

(c)

ENMs Concentration		n-Ag (µg/L)				
		50	20	10	5	0
P25 (mg/L)	0.5	277 (±17)	332 (±12)	445 (±10)	306 (±3)	546 (±28)
	0.2	426 (±7)	361 (±13)	438 (±9)	556 (±11)	503 (±3)
	0.1	433 (±41)	399 (±5)	423 (±21)	411 (±9)	466 (±34)

Figure S11. Aggregate size (nm) of (a) n-TiO_2 P25 in LMW and (b) mixtures with n-Ag mixtures under light and (c) in dark in LMW for 2 hours.

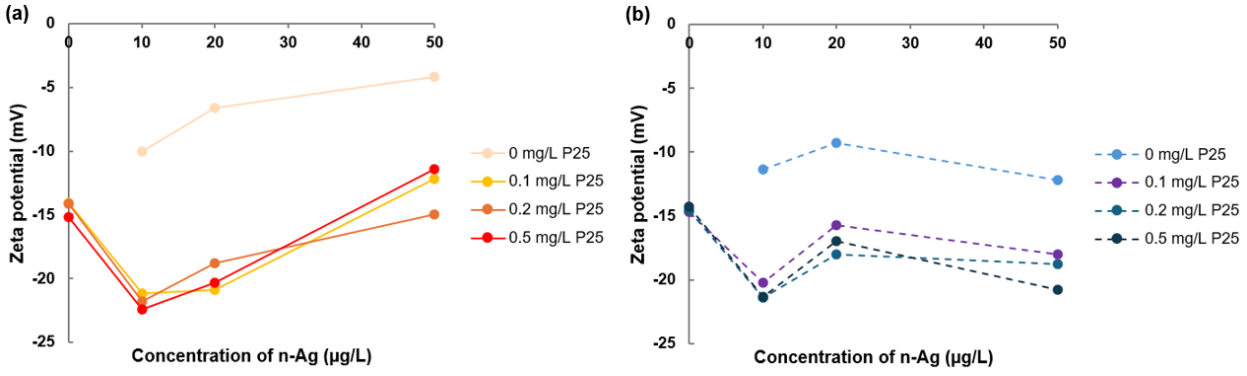

Figure S12. Zeta potential of n-TiO_2 P25 and n-Ag and their mixtures in LMW (a) under light and (b) in dark for 2 hours.

Reference

1. Raza, S.; Folga, M.; Los, M.; Foltynowicz, Z.; Paczesny, J., The Effect of Zero-Valent Iron Nanoparticles (nZVI) on Bacteriophages. *Viruses* **2022,** *14*, (5).
2. Cheng, R.; Zhang, Y. Y.; Zhang, T.; Hou, F.; Cao, X. X.; Shi, L.; Jiang, P. W.; Zheng, X.; Wang, J. L., The inactivation of bacteriophages MS2 and PhiX174 by nanoscale zero-valent iron: Resistance difference and mechanisms. *Frontiers of Environmental Science & Engineering* **2022,** *16*, (8).
3. Cheng, R.; Li, G. Q.; Cheng, C.; Liu, P.; Shi, L.; Ma, Z.; Zheng, X., Removal of bacteriophage f2 in water by nanoscale zero-valent iron and parameters optimization using response surface methodology. *Chem Eng J* **2014,** *252*, 150-158.
4. Cheng, R.; Li, G. Q.; Shi, L.; Xue, X. Y.; Kang, M.; Zheng, X., The mechanism for bacteriophage f2 removal by nanoscale zero-valent iron. *Water Research* **2016,** *105*, 429-435.
5. Yuan, D. H.; Zhai, L. X.; Zhang, X. Y.; Cui, Y. Q.; Wang, X. Y.; Zhao, Y. X.; Xu, H. D.; He, L. S.; Yan, C. L.; Cheng, R.; Kou, Y. Y.; Li, J. Q., Study on the characteristics and mechanism of bacteriophage MS2 inactivated by bacterial cellulose supported nanoscale zero-valent iron. *J Clean Prod* **2020,** *270*.
6. Cheng, R.; Kang, M.; Zhuang, S.; Wang, S.; Zheng, X.; Pan, X.; Shi, L.; Wang, J., Removal of bacteriophage f2 in water by Fe/Ni nanoparticles: Optimization of Fe/Ni ratio and influencing factors. *Sci Total Environ* **2019,** *649*, 995-1003.
7. Stachurska, X.; Cendrowski, K.; Pachnowska, K.; Piegat, A.; Mijowska, E.; Nawrotek, P., Nanoparticles Influence Lytic Phage T4-like Performance In Vitro. *Int J Mol Sci* **2022,** *23*, (13).
8. Han, X.; Lv, P.; Wang, L. G.; Long, F.; Ma, X. L.; Liu, C.; Feng, Y. J.; Yang, M. F.; Xiao, X., Impact of nano-TiO_2 on horizontal transfer of resistance genes mediated by filamentous phage transduction. *Environ Sci-Nano* **2020,** *7*, (4), 1214-1224.
9. Gilcrease, E.; Williams, R.; Goel, R., Evaluating the effect of silver nanoparticles on bacteriophage lytic infection cycle-a mechanistic understanding. *Water Research* **2020,** *181*.
10. Zhang, Q.; Zhou, H.; Jiang, P.; Wu, L.; Xiao, X., Silver nanoparticles facilitate phage-borne resistance gene transfer in planktonic and microplastic-attached bacteria. *J Hazard Mater* **2024,** *469*, 133942.
11. Guo, J. H.; Gao, S. H.; Lu, J.; Bond, P. L.; Verstraete, W.; Yuan, Z. G., Copper Oxide Nanoparticles Induce Lysogenic Bacteriophage and Metal-Resistance Genes in PAO1. *Acs Appl Mater Inter* **2017,** *9*, (27), 22298-22307.
12. Rao, G. Y.; Brastad, K. S.; Zhang, Q. Y.; Robinson, R.; He, Z.; Li, Y., Enhanced disinfection of Escherichia coli and bacteriophage MS2 in water using a copper and silver loaded titanium dioxide nanowire membrane. *Frontiers of Environmental Science & Engineering* **2016,** *10*, (4).
13. You, J.; Zhang, Y.; Hu, Z., Bacteria and bacteriophage inactivation by silver and zinc oxide nanoparticles. *Colloids and Surfaces B: Biointerfaces* **2011,** *85*, 161-167.
14. Nickel, A.; Pedulla, M.; Kasinath, R., The effect of nanoparticles on bacteriophage infections. In *NSTI-Nanotech 2010*, 2010; Vol. 3.
15. Xiao, X.; Ma, X. L.; Han, X.; Wu, L. J.; Liu, C.; Yu, H. Q., TiO(2) photoexcitation promoted horizontal transfer of resistance genes mediated by phage transduction. *Sci Total Environ* **2021,** *760*, 144040.
16. Zhang, Q. R.; Zhou, H. X.; Qiao, J.; Jiang, P.; Xiao, X., New insight into nanomaterial-mediated dissemination of phage-borne resistance genes: Roles of humic acid and illumination. *Chem Eng J* **2024,** *486*.
17. Syngouna, V. I.; Chrysikopoulos, C. V., Inactivation of MS2 bacteriophage by titanium dioxide nanoparticles in the presence of quartz sand with and without ambient light. *J Colloid Interf Sci* **2017,** *497*, 117-125.
18. Lee, J. E.; Ko, G., Norovirus and MS2 inactivation kinetics of UV-A and UV-B with and without TiO_2. *Water Research* **2013,** *47*, (15), 5607-5613.

19. Koizumi, Y.; Taya, M., Kinetic evaluation of biocidal activity of titanium dioxide against phage MS2 considering interaction between the phage and photocatalyst particles. *Biochem Eng J* **2002,** *12*, (2), 107-116.
20. Zheng, X.; Shen, Z. P.; Cheng, C.; Shi, L.; Cheng, R.; Yuan, D. H., Photocatalytic disinfection performance in virus and virus/bacteria system by Cu-TiO_2 nanofibers under visible light. *Environmental Pollution* **2018,** *237*, 452-459.
21. Wu, S. S.; Wells, G.; Gray, K. A., Engineered nanomaterials exert sublethal bacterial stress at very low doses: Effects of concentration, light, and media on cell membrane permeability. *Science of the Total Environment* **2024,** *948*.
22. Tong, T.; Binh, C. T.; Kelly, J. J.; Gaillard, J. F.; Gray, K. A., Cytotoxicity of commercial nano-TiO2 to Escherichia coli assessed by high-throughput screening: effects of environmental factors. *Water Res* **2013,** *47*, (7), 2352-62.
23. Viveiros, M.; Dupont, M.; Rodrigues, L.; Couto, I.; Davin-Regli, A.; Martins, M.; Pages, J. M.; Amaral, L., Antibiotic stress, genetic response and altered permeability of E. coli. *PLoS One* **2007,** *2*, (4), e365.